Supporting Information

Co-substitution in $Ca_{1-x}Y_xAl_{12-x}Mg_xO_{19}$ phosphors: Local structure evolution, photoluminescence tuning and application for plant growth LEDs

Yinjian Zheng, [a] *Haiming Zhang,* [a] *Haoran Zhang,* [a] *Zhiguo Xia,* [b] *Yingliang Liu,* [a] *Maxim S. Molokeev,* [c,d] *Bingfu Lei* [*,a]

[a] Guangdong Provincial Engineering Technology Research Center for Optical Agricultural, College of Materials and Energy, South China Agricultural University, Guangzhou 510642, China
[b] School of Materials Sciences and Engineering, University of Science and Technology Beijing, Beijing 100083, China
[c] Laboratory of Crystal Physics, Kirensky Institute of Physics, Federal Research Center KSC SB RAS, Krasnoyarsk 660036, Russia
[d] Department of Physics, Far Eastern State Transport University, Khabarovsk, 680021 Russia

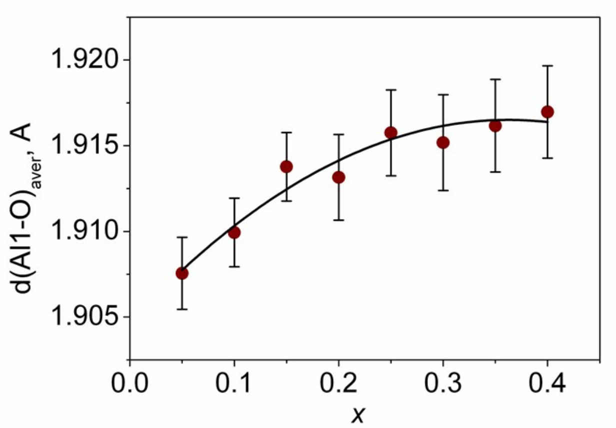

a)

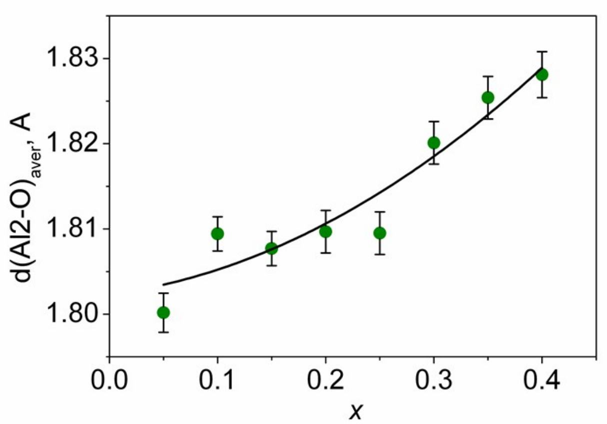

b)

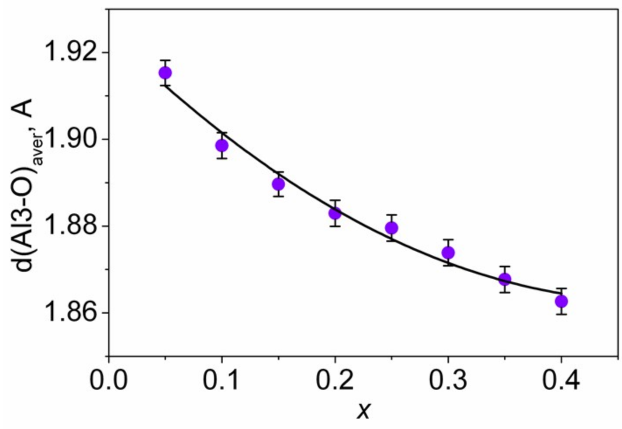

c)

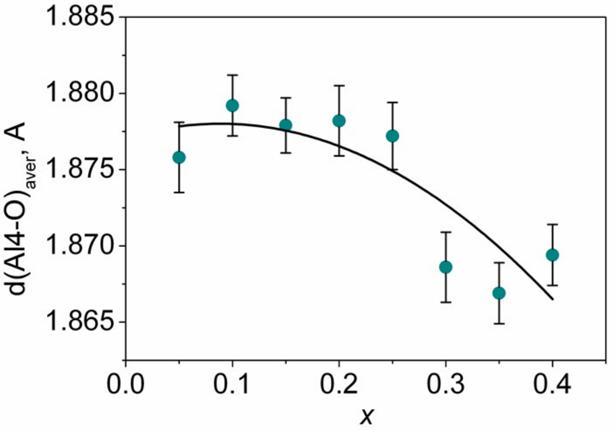

d)

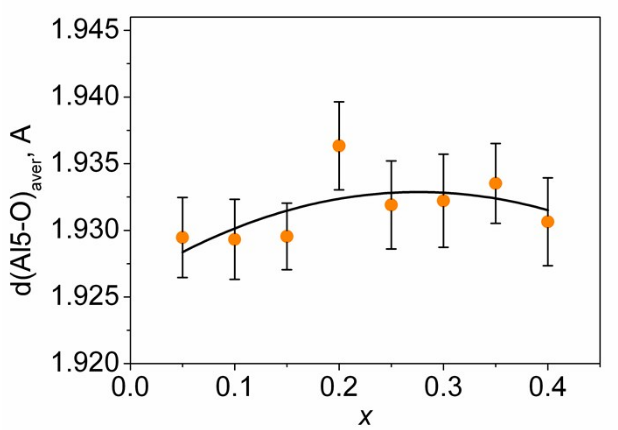

e)

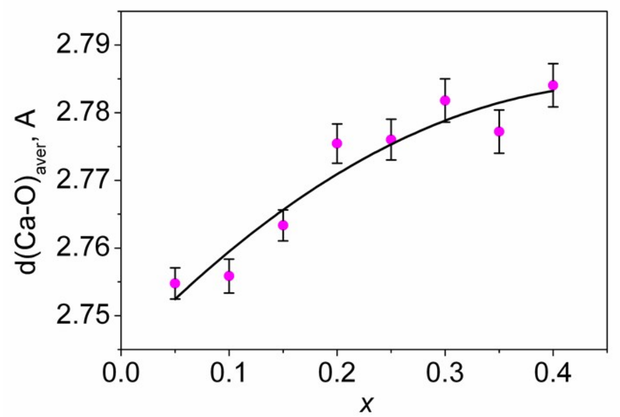

f)

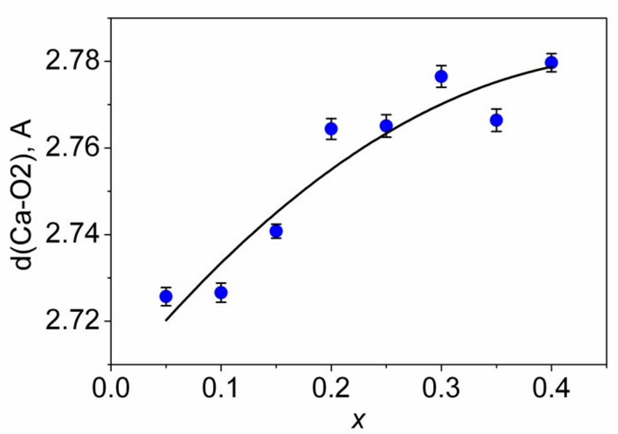

g)

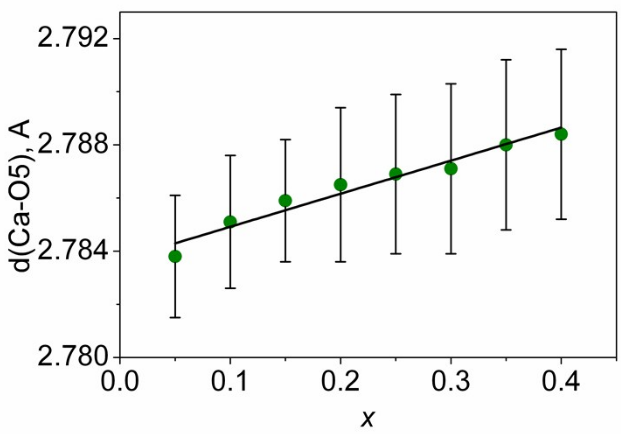

h)

Figure 1S. Dependences of main bond lengths per *x*: average d(Al1-O) (a); average d(Al2-O) (b); average d(Al3-O) (c); average d(Al4-O) (d); average d(Al5-O) (e); average d(Ca-O) (f); d(Ca-O2) (g); d(Ca-O5) (h).

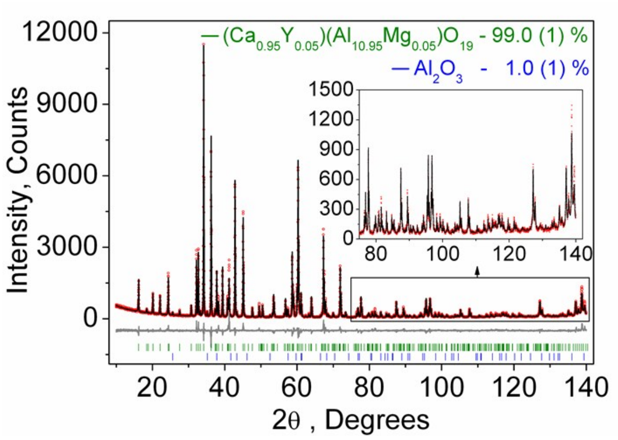
— (Ca0.95Y0.05)(Al10.95Mg0.05)O19 - 99.0 (1) %
— Al2O3 - 1.0 (1) %
Intensity, Counts
2θ , Degrees

a)

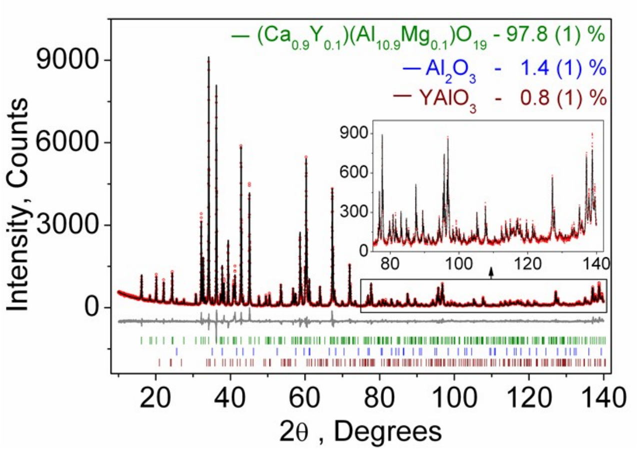
— (Ca0.9Y0.1)(Al10.9Mg0.1)O19 - 97.8 (1) %
— Al2O3 - 1.4 (1) %
— YAlO3 - 0.8 (1) %
Intensity, Counts
2θ , Degrees

b)

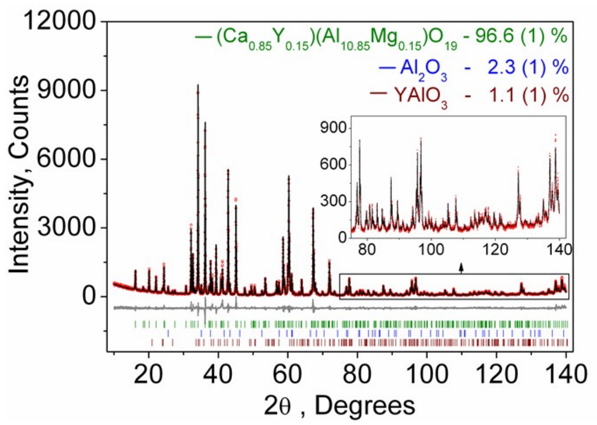
— (Ca0.85Y0.15)(Al10.85Mg0.15)O19 - 96.6 (1) %
— Al2O3 - 2.3 (1) %
— YAlO3 - 1.1 (1) %
Intensity, Counts
2θ , Degrees

c)

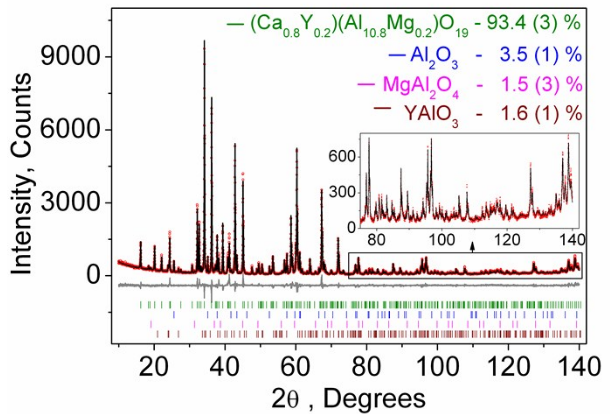
— (Ca0.8Y0.2)(Al10.8Mg0.2)O19 - 93.4 (3) %
— Al2O3 - 3.5 (1) %
— MgAl2O4 - 1.5 (3) %
— YAlO3 - 1.6 (1) %
Intensity, Counts
2θ , Degrees

d)

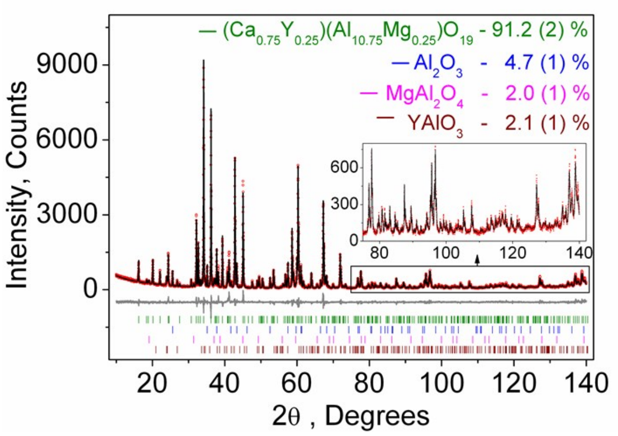
— (Ca0.75Y0.25)(Al10.75Mg0.25)O19 - 91.2 (2) %
— Al2O3 - 4.7 (1) %
— MgAl2O4 - 2.0 (1) %
— YAlO3 - 2.1 (1) %
Intensity, Counts
2θ , Degrees

e)

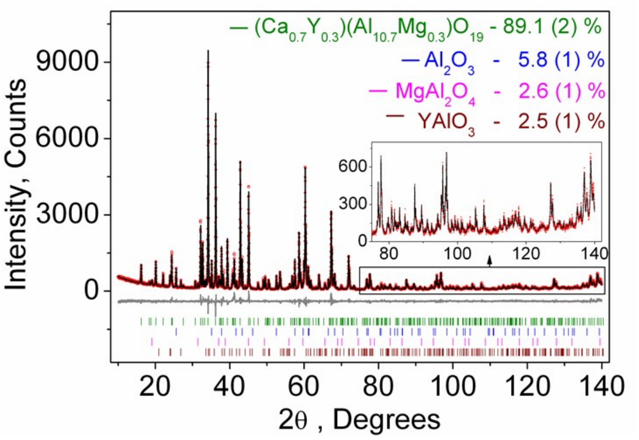
— (Ca0.7Y0.3)(Al10.7Mg0.3)O19 - 89.1 (2) %
— Al2O3 - 5.8 (1) %
— MgAl2O4 - 2.6 (1) %
— YAlO3 - 2.5 (1) %
Intensity, Counts
2θ , Degrees

f)

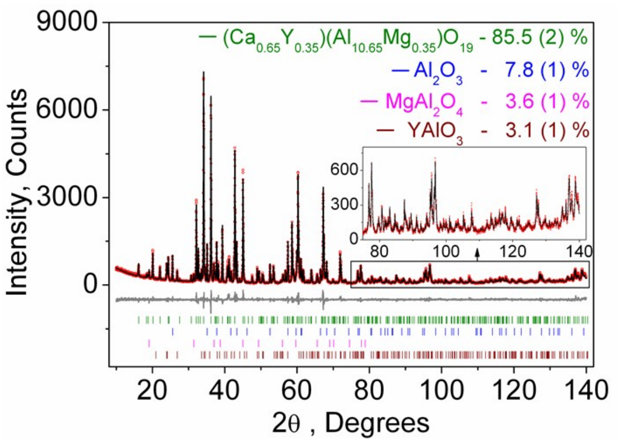

g)

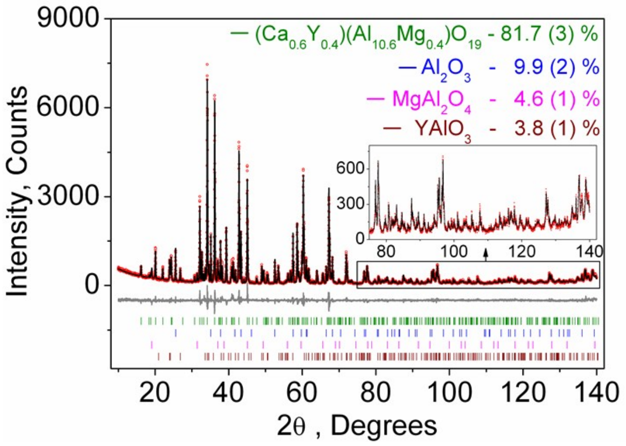

h)

Figure 2S. Difference Rietveld plot of $(Ca_{1-x}Y_x)(Al_{12-x}Mg_x)O_{19}$:$Mn^{4+}$: a) $x = 0.05$; b) $x = 0.1$; c) $x = 0.15$; d) $x = 0.2$; e) $x = 0.25$; f) $x = 0.3$; g) $x = 0.35$; h) $x = 0.4$. Bragg peaks of different phases are marked by colored sticks.

Table 1S. Fractional atomic coordinates and isotropic displacement parameters (Å^2) of $(Ca_{1-x}Y_x)(Al_{12-x}Mg_x)O_{19}$:$Mn^{4+}$

	x	y	z	B_{iso}	Occ.
			$x = 0.05$		
Ca	1/3	2/3	3/4	1.33 (6)	0.943 (5)
Y	1/3	2/3	3/4	1.33 (6)	0.057 (3)
Al1	0.16870 (15)	0.3374 (3)	-0.10935 (3)	0.70 (3)	1
Al2	1/3	2/3	0.02835 (7)	0.70 (3)	0.972 (2)
Mg2	1/3	2/3	0.02835 (7)	0.70 (3)	0.028 (2)
Al3	1/3	2/3	0.19071 (6)	0.70 (3)	1
Al4	0	0	0	0.70 (3)	1
Al5	0	0	1/4	0.70 (3)	1
O1	0.1559 (3)	0.3118 (5)	0.05188 (7)	1.00 (3)	1
O2	0.5041 (3)	1.0082 (7)	0.14879 (7)	1.00 (3)	1
O3	1/3	2/3	-0.0539 (1)	1.00 (3)	1
O4	0	0	0.1492 (1)	1.00 (3)	1
O5	0.1799 (4)	0.3598 (8)	1/4	1.00 (3)	1
			$x = 0.1$		
Ca	1/3	2/3	0.75	1.17 (5)	0.947 (4)
Y	1/3	2/3	0.75	1.17 (5)	0.053 (4)

Al1	0.1688 (1)	0.3375 (3)	-0.10929 (3)	0.75 (3)	1
Al2	1/3	2/3	0.02811 (7)	0.75 (3)	0.974 (2)
Mg2	1/3	2/3	0.02811 (7)	0.75 (3)	0.026 (2)
Al3	1/3	2/3	0.19068 (7)	0.75 (3)	1
Al4	0	0	0	0.75 (3)	1
Al5	0	0	1/4	0.75 (3)	1
O1	0.1552 (3)	0.3105 (5)	0.05246 (7)	1.00 (3)	1
O2	0.5036 (3)	1.0071 (7)	0.14946 (7)	1.00 (3)	1
O3	1/3	2/3	-0.0543 (1)	1.00 (3)	1
O4	0	0	0.1503 (1)	1.00 (3)	1
O5	0.1805 (4)	0.3611 (7)	1/4	1.00 (3)	1
			$x = 0.15$		
Ca	1/3	2/3	3/4	1.30 (6)	0.912 (5)
Y	1/3	2/3	3/4	1.30 (6)	0.088 (5)
Al1	0.1686 (3)	0.3371 (3)	-0.10933 (4)	0.78 (3)	1
Al2	1/3	2/3	0.02811 (8)	0.78 (3)	0.956 (2)
Mg2	1/3	2/3	0.02811 (8)	0.78 (3)	0.044 (2)
Al3	1/3	2/3	0.19069 (7)	0.78 (3)	1
Al4	0	0	0	0.78 (3)	1
Al5	0	0	1/4	0.78 (3)	1
O1	0.1555 (3)	0.3109 (5)	0.05237 (8)	1.00 (4)	1
O2	0.5038 (4)	1.0076 (7)	0.14942 (8)	1.00 (4)	1
O3	1/3	2/3	-0.0543 (2)	1.00 (4)	1
O4	0	0	0.1504 (1)	1.00 (4)	1
O5	0.1805 (4)	0.3610 (7)	1/4	1.00 (4)	1
			$x = 0.2$		
Ca	1/3	2/3	3/4	1.49 (6)	0.869 (5)
Y	1/3	2/3	3/4	1.49 (6)	0.131 (5)
Al1	0.1686 (2)	0.3372 (3)	-0.10946 (4)	0.80 (3)	1
Al2	1/3	2/3	0.02821 (8)	0.80 (3)	0.934 (2)
Mg2	1/3	2/3	0.02821 (8)	0.80 (3)	0.066 (2)
Al3	1/3	2/3	0.19063 (7)	0.80 (3)	1
Al4	0	0	0	0.80 (3)	1

Al5	0	0	1/4	0.80 (3)	1
O1	0.1563 (3)	0.3127 (6)	0.05240 (8)	1.00 (4)	1
O2	0.5033 (4)	1.0066 (7)	0.14895 (8)	1.00 (4)	1
O3	1/3	2/3	-0.0543 (2)	1.00 (4)	1
O4	0	0	0.1499 (2)	1.00 (4)	1
O5	0.1803 (4)	0.3606 (8)	1/4	1.00 (4)	1
			x = 0.25		
Ca	1/3	2/3	3/4	1.46 (6)	0.855 (5)
Y	1/3	2/3	3/4	1.46 (6)	0.145 (5)
Al1	0.16867 (15)	0.3374 (3)	-0.10938 (4)	0.76 (3)	1
Al2	1/3	2/3	0.02826 (8)	0.76 (3)	0.928 (2)
Mg2	1/3	2/3	0.02826 (8)	0.76 (3)	0.072 (2)
Al3	1/3	2/3	0.19065 (8)	0.76 (3)	1
Al4	0	0	0	0.76 (3)	1
Al5	0	0	1/4	0.76 (3)	1
O1	0.1561 (3)	0.3122 (6)	0.05246 (8)	1.00 (4)	1
O2	0.5039 (4)	1.0078 (7)	0.14926 (8)	1.00 (4)	1
O3	1/3	2/3	-0.05436 (16)	1.00 (4)	1
O4	0	0	0.15036 (15)	1.00 (4)	1
O5	0.1809 (4)	0.3617 (8)	1/4	1.00 (4)	1
			x = 0.3		
Ca	1/3	2/3	3/4	1.50 (6)	0.827 (5)
Y	1/3	2/3	3/4	1.50 (6)	0.173 (5)
Al1	0.1687 (2)	0.3374 (3)	-0.10939 (4)	0.76 (3)	1
Al2	1/3	2/3	0.02829 (8)	0.76 (3)	0.913 (2)
Mg2	1/3	2/3	0.02829 (8)	0.76 (3)	0.087 (2)
Al3	1/3	2/3	0.19059 (7)	0.76 (3)	1
Al4	0	0	0	0.76 (3)	1
Al5	0	0	1/4	0.76 (3)	1
O1	0.1550 (3)	0.3100 (6)	0.05253 (8)	1.00 (4)	1
O2	0.5040 (3)	1.0079 (7)	0.14927 (8)	1.00 (4)	1
O3	1/3	2/3	-0.0547 (2)	1.00 (4)	1
O4	0	0	0.1503 (2)	1.00 (4)	1

O5	0.1807 (4)	0.3614 (8)	1/4	1.00 (4)	1
			$x = 0.35$		
Ca	1/3	2/3	3/4	1.39 (6)	0.836 (5)
Y	1/3	2/3	3/4	1.39 (6)	0.164 (5)
Al1	0.1688 (2)	0.3376 (3)	-0.10914 (4)	0.81 (3)	1
Al2	1/3	2/3	0.02801 (9)	0.81 (3)	0.918 (2)
Mg2	1/3	2/3	0.02801 (9)	0.81 (3)	0.082 (2)
Al3	1/3	2/3	0.19035 (8)	0.81 (3)	1
Al4	0	0	0	0.81 (3)	1
Al5	0	0	1/4	0.81 (3)	1
O1	0.1543 (3)	0.3086 (6)	0.05267 (9)	1.00 (4)	1
O2	0.5041 (4)	1.0081 (7)	0.15007 (9)	1.00 (4)	1
O3	1/3	2/3	-0.05480 (17)	1.00 (4)	1
O4	0	0	0.15076 (17)	1.00 (4)	1
O5	0.1817 (4)	0.3634 (8)	1/4	1.00 (4)	1
			$x = 0.4$		
Ca	1/3	2/3	3/4	1.46 (7)	0.789 (5)
Y	1/3	2/3	3/4	1.46 (7)	0.211 (5)
Al1	0.1693 (2)	0.3385 (4)	-0.10912 (4)	0.85 (5)	1
Al2	1/3	2/3	0.0279 (1)	0.85 (5)	0.894 (3)
Mg2	1/3	2/3	0.0279 (1)	0.85 (5)	0.105 (3)
Al3	1/3	2/3	0.19030 (9)	0.85 (5)	1
Al4	0	0	0	0.85 (5)	1
Al5	0	0	1/4	0.85 (5)	1
O1	0.1548 (3)	0.3095 (7)	0.05281 (9)	1.00 (6)	1
O2	0.5048 (4)	1.0096 (8)	0.15027 (9)	1.00 (6)	1
O3	1/3	2/3	-0.0548 (2)	1.00 (6)	1
O4	0	0	0.1508 (2)	1.00 (6)	1
O5	0.1815 (4)	0.3630 (8)	1/4	1.00 (6)	1

Table 2S. Main bond lengths (Å) of $(Ca_{1-x}Y_x)(Al_{12-x}Mg_x)O_{19}$:$Mn^{4+}$

$x = 0.05$			
(Ca/Y)—O2^{i}	2.713 (2)	(Al2/Mg2)—O3	1.801 (3)

(Ca/Y)—O5^{ii}	2.783 (3)	Al3—O2	1.884 (3)
Al1—O1^{iii}	2.010 (2)	Al3—O5	1.967 (3)
Al1—O2^{iv}	1.797 (2)	Al4—O1	1.883 (2)
Al1—O3	1.997 (2)	Al5—O4	2.208 (3)
Al1—O4^{iii}	1.844 (2)	Al5—O5	1.733 (4)
(Al2/Mg2)—O1	1.785 (3)		
x = 0.1			
(Ca/Y)—O2^{i}	2.704 (2)	(Al2/Mg2)—O3	1.804 (3)
(Ca/Y)—O5^{ii}	2.784 (3)	Al3—O2	1.872 (3)
Al1—O1^{iii}	1.999 (2)	Al3—O5	1.963 (3)
Al1—O2^{iv}	1.807 (2)	Al4—O1	1.886 (2)
Al1—O3	1.991 (2)	Al5—O4	2.184 (3)
Al1—O4^{iii}	1.857 (2)	Al5—O5	1.739 (3)
(Al2/Mg2)—O1	1.796 (2)		
x = 0.15			
(Ca/Y)—O2^{i}	2.704 (2)	(Al2/Mg2)—O3	1.804 (4)
(Ca/Y)—O5^{ii}	2.784 (3)	Al3—O2	1.874 (3)
Al1—O1^{iii}	2.001 (2)	Al3—O5	1.963 (3)
Al1—O2^{iv}	1.806 (2)	Al4—O1	1.886 (2)
Al1—O3	1.993 (2)	Al5—O4	2.180 (3)
Al1—O4^{iii}	1.857 (2)	Al5—O5	1.739 (4)
(Al2/Mg2)—O1	1.794 (3)		
x = 0.2			
(Ca/Y)—O2^{i}	2.715 (2)	(Al2/Mg2)—O3	1.806 (4)
(Ca/Y)—O5^{ii}	2.785 (3)	Al3—O2	1.875 (3)
Al1—O1^{iii}	2.005 (2)	Al3—O5	1.965 (3)
Al1—O2^{iv}	1.802 (2)	Al4—O1	1.893 (2)
Al1—O3	1.994 (2)	Al5—O4	2.191 (3)
Al1—O4^{iii}	1.850 (2)	Al5—O5	1.737 (4)
(Al2/Mg2)—O1	1.786 (3)		
x = 0.25			
(Ca/Y)—O2^{i}	2.706 (2)	(Al2/Mg2)—O3	1.808 (4)

(Ca/Y)—O5^{ii}	2.785 (3)	Al3—O2	1.877 (3)
Al1—O1^{iii}	2.003 (2)	Al3—O5	1.961 (3)
Al1—O2^{iv}	1.803 (2)	Al4—O1	1.893 (2)
Al1—O3	1.992 (3)	Al5—O4	2.181 (3)
Al1—O4^{iii}	1.857 (2)	Al5—O5	1.743 (4)
(Al2/Mg2)—O1	1.788 (3)		
$x = 0.3$			
(Ca/Y)—O2^{i}	2.705 (2)	(Al2/Mg2)—O3	1.816 (4)
(Ca/Y)—O5^{ii}	2.785 (3)	Al3—O2	1.877 (3)
Al1—O1^{iii}	1.999 (2)	Al3—O5	1.963 (3)
Al1—O2^{iv}	1.803 (2)	Al4—O1	1.885 (2)
Al1—O3	1.987 (2)	Al5—O4	2.182 (3)
Al1—O4^{iii}	1.856 (2)	Al5—O5	1.741 (4)
(Al2/Mg2)—O1	1.798 (3)		
$x = 0.35$			
(Ca/Y)—O2^{i}	2.691 (3)	(Al2/Mg2)—O3	1.812 (4)
(Ca/Y)—O5^{ii}	2.786 (3)	Al3—O2	1.867 (3)
Al1—O1^{iii}	1.991 (2)	Al3—O5	1.960 (3)
Al1—O2^{iv}	1.813 (2)	Al4—O1	1.882 (3)
Al1—O3	1.982 (3)	Al5—O4	2.172 (4)
Al1—O4^{iii}	1.864 (2)	Al5—O5	1.751 (4)
(Al2/Mg2)—O1	1.808 (3)		
$x = 0.4$			
(Ca/Y)—O2^{i}	2.682 (3)	(Al2/Mg2)—O3	1.809 (5)
(Ca/Y)—O5^{ii}	2.786 (4)	Al3—O2	1.871 (4)
Al1—O1^{iii}	1.993 (2)	Al3—O5	1.962 (3)
Al1—O2^{iv}	1.811 (2)	Al4—O1	1.887 (3)
Al1—O3	1.978 (3)	Al5—O4	2.170 (4)
Al1—O4^{iii}	1.869 (3)	Al5—O5	1.750 (4)
(Al2/Mg2)—O1	1.806 (3)		

Symmetry codes: (i) $-x+1$, $-x+y$, $-z+1$; (ii) $-x$, $-x+y$, $-z+1$; (iii) $-x$, $-x+y$, $-z$; (iv) $-x+1$, $-x+y$, $-z$.

LED light applied in plant growth

Light quality is an important component among the environmental factors that distinctly effect plant growth and development. At presented, at least four photoreceptors gene family in plant control the plant lifecycle had been accepted by public.[1] The phytochrome receptor that monitor the red (R) and far-red (FR) regions of the light spectrum, and can significantly affect the germination, hypocotyl development, photosynthesis and so on.[2]

Phytochromes were the first light-sensing molecules discovered in plants and then identified in a broad spectrum of eukaryotic and prokaryotic phyla.[3]. Phytochromes can be either in an inactive or active form, and gene familyhave PhyA, PhyB, PhyC, PhyD and PhyE five speices. The R:FR ratio is often used to quantify spectral photon flux distribution in the R and FR wavelengths.[4]

Brassica is a large number leaf vegetables cultivations in plant, expecially, the Arabidopsis as a model plant has been extensive study in plant, Green and red-leaf pak-choi and flowering Chinese cabbage, a leafy Chinese vegetable, and the gene group of these species are similar to Arabidopsis. Cucumber is an economically important horticultural crop and highly sensitive to salinity, especially at the seedling stage.[5] In this study, the reason why used the three brassica species want to exclude from the difference on cultivation, and find the different red/far-red percentage how to effect the morphology of cucumber seeding. According to artificial LED light with phosphor (when x =0, 0.1, 0.4) radio these plants, then get a credible artificial illumination in yield of plant lighting.

Materials and method

Cultivated condition

The typical $Ca_{1-x}Y_xAl_{12-x}Mg_xO_{19}:Mn^{4+}$ (x = 0, 0.10, 0.40) phosphor artificial illumination, which is named T1, T2 and T3, respectively. These plant cultivated into cabinet, the light intensity radio on the plant was 50μmol·m^{-2}·s^{-1}, 12 hours (on/off), the temperature was 26 ℃, the air humidity was 75 %. The seed was soaking two hours, then seeds were sowed in sponge block (2 cm * 2 cm * 2 cm), after seven days cultivated with nutrient solution ($CaNO_3$ 236.25 mg/L, KNO_3 151.75 mg/L, NH_4PO_4 28.75 mg/L, $MgSO_4$ 123.25 mg/L, pH ≈6.0).

The method of biomass and morphology

The plants were harvested for biomass and morphology measurements. The fresh and dry weight of shoot and root were measured, the dry weight was determined after 48 h at 70 ◦C in drying oven.

The method of bio-active phytochemistry

The content of soluble sugars was measured by the method of sulfuric acid anthrone.[6]. 0.05 g fresh shoot were put into a test tube, 5 mL distilled water was added and mixed. After 30 min in a water bath at 85 °C, the supernatent was collected. This step was repeated twice, and distilled water was added to a volume of 10 mL. The soluble sugar content was determined at 620 nm by UV-spectrophotometer.

Soluble proteins were measured by Coomassie brilliant blue method.[7] 0.05 g fresh shoot were ground up in a mortar with liquid nitrogen, to which 3 mL of a phosphate-buffered solution (pH 7.0) was added. The extract was centrifuged at 13,000 × g for 15 min at 4 °C, and 0.1 mL of the supernatant was combined with 4.9 mL Coomassie brilliant blue G-250 solution (0.1 g/L). After 2 min, the soluble protein content was determined at 595 nm by UV-spectrophotometer.

The content of free amino acid was measured colorimetrically.[8] 1.0 g fresh shoot were ground up, and then 5 mL of acetic acid washed samples pure into 100 mL volumetric flask, 100 mL deionized water was added, prepared for measurement. 1.0 mL extracting solution, 10 mL deionized water, 0.1 mL ascorbic acid solution and Hydrated indene ketone solution were boiling for 15 min, 20 mL 60% ethanol was added, the free amino acid was measured at 570 nm by UV-spectrophotometer.

The photosynthesis index was method by li-6400 photosynthesis system.

Statistical analysis

All the assays were performed in triplicates. Significant differences among the treatments were determined by analysis of variance (ANOVA) followed by Duncan multiple range tests of SPSS 17.0, the Table and Graphic was made by word 2013 and OriginPro 9.0.

Result and discussion

The green-leaf pak-choi, red-leaf pak-choi and flowering Chinese cabbage act as plant model for study the photosynthesis and bio-active metabolism of plant, which were cultivated under different red/far-red percentage radio condition.

From figure 3S, three brassica species under different treatments had similar changed tendency, with R:FR radio decreased, the biomass of these plants significantly decreased, and the red-leaf pak-choi leaf color also deepened. The petiole and leaf area is stretch with red intensity increasing. In arabidopsis, petiole elongation is stimulated by low R:FR radio.[9] In rice, the three phytochromes contribute to multiple steps control expression of the GA biosynthesis gene OsGA3ox2 to regulate the internode elongation.[10] Our results also have the similar phenomenon.

Get further study, the photosynthesis and bio-active phytochemistry was be measured by us. Based on the theory of R:FR ratio can indirectly change photosynthesis at the scale of the whole plant. In arabidopsis, lower R:FR radio can upregulated PhyB, and phyB-overexpressing mutants showed that reduced expression of PhyB decreases stomatal opening, and can either decrease or increase CO_2 stomatal conductance.[11] In our study, the three brassica species under higher R:FR radio (T1) had the lowest Gs (Figure 4Sb, Figure 5Sb and Figure 6Sb) among treatments, this result is similar to above conclusion on arabidopsis. Because of the Gs opening with far-red radio-increasing, the Evap of plant also increasing. Obtain the data from Figure 4Sd, Figure 3Sd and Figure 4Sd, the plant Ci was significantly decreased with FR radio-increasing, while, the Pn in plant had the opposite changed tendency from Ci, the reason is to be the higher far-red radio light is a stress for plant growth, the plant consumed more energy to tolerant the demange. The soluble sugars is the production of photosynthesis, the soluble sugars in three brassica species had the same changed tendency from Pn, this result can also support above conclusion. The other bio-active phytochemistry measured in study had no significantly difference among treatments.

Select the cucumber seeding as a model want to found how to the different R:FR radio effect the plant germination and morphology.

Seed germination is a crucial event in plant life. It is highly regulated by light and temperature. Seed germination is light-sensitive mechanism based on the relative abundance of red and far-red perceived by phytochromes.[12] FR light is abundant, and PhyB-dependent germination is blocked: FR activates PhyA and allows for germination in negatively photoblastic seeds.[13] The germination rate of cucumber was obtain from Figure 10S, which was presented remarkably inhabited with emission far-red ratio-increased, During the cucumber in 10-days-old period, added far-red wavelength treatments delayed the euphylla appeared, and the euphylla was distinctly curlied with far-red ratio-increased. This result accordance with above conclusion.

After seed 10 days, all cucumber seeding moved into sunlight condition cultivated 10 days, harvested at 20-days-old, then measured the seedling indexs, photosynthesis and obtain the morphology picture of seeding.

In dicotyledonous species, petiole elongation is stimulated by low R:FR, This response depends on PhyB, and the PhyB contribution of PIF4 and PIF5 in plant, which have the inhibit function on euphylla area, stem diameter, plant height and Hypocotyl length.[14] Generally, the morphology statistical data of seeding are described in Table S1. Different treatments can significant effect the growth of cucumber seeding, T2 had the highest fresh/dry weight in plant (overground and underground), T1 had the highest stem diameter and the shortest hypocotyl length, the Figure S8 also presented the same changed tendency.

The photosynthesis data (Evap, Gs, Pn and Ci) of cucumber seeding, which were treated with different percentage emit far-red light intensity, obtain in Figure 11S, the Evap of cucumber under T1 and T2 had no significant difference, while the T3 had the lowest Evap. The Gs had the opposite data from Evap, this result should be explain that the red light (660 nm) is the characteristic absorption peak of photosynthesis, added lower far-red ratio can improve carbohydrate accumulate in plant, the figure S9c, the Pn can clearly presented photosynthesis production quantity. From Table S1, the results fresh and dry weight in plant had the same as the Pn. Hence, above results can conclusion that higher far-red light can decrease Evap and increased Gs for inhibit the Pn accumulate in cucumber seeding.

Conclusion

Above analysis, we can not hesitate to say, the red to far-red ratio-tunable Ca_{1-}

$_xY_xAl_{12-x}Mg_xO_{19}:Mn^{4+}$ phosphor is applied to plant growth have excellently effect.

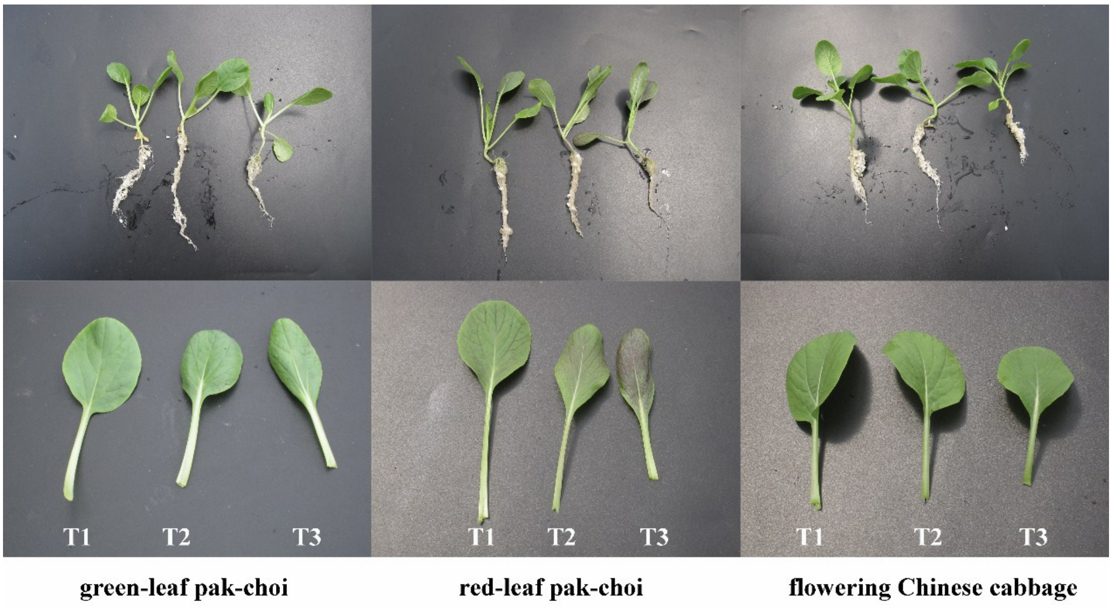

Figure 3S. The morphology of green-leaf pak-choi, red-leaf pak-choi and flowering Chinese cabbage.

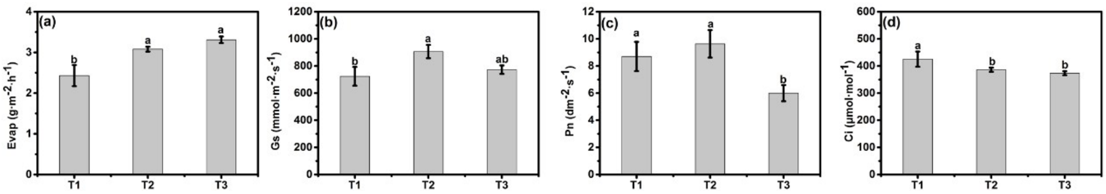

Figure 4S. The photosynthesis parameters of green-leaf pak-choi under red:far-red radio. (a) Transportation Rate (Evap), (b) stomatal conductance (Gs), (c) Photosynthesis Rate (Pn), (d) intercellular CO_2 concentration (Ci). Different letters indicate significant differences between treatments (a< 0.05).

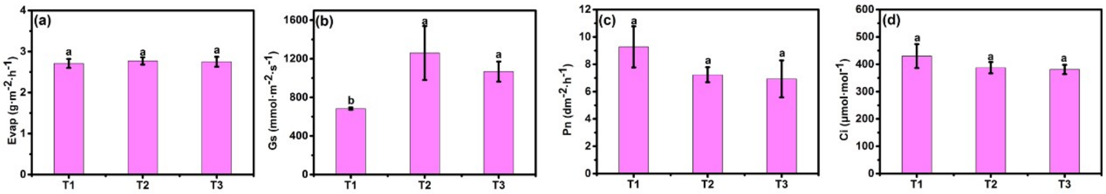

Figure 5S. The photosynthesis parameters of red-leaf pak-choi under red:far-red radio. (a) Transportation Rate (Evap), (b) stomatal conductance (Gs), (c) Photosynthesis Rate (Pn), (d) intercellular CO_2 concentration (Ci). Different letters indicate significant differences between treatments (a< 0.05).

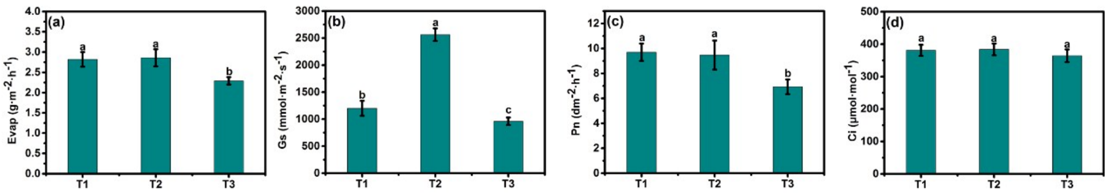

Figure 6S. The photosynthesis parameters of flowering Chinese cabbage under red:far-red radio. (a) Transportation Rate (Evap), (b) stomatal conductance (Gs), (c) Photosynthesis Rate (Pn), (d) intercellular CO_2 concentration (Ci). Different letters indicate significant differences between treatments (a< 0.05).

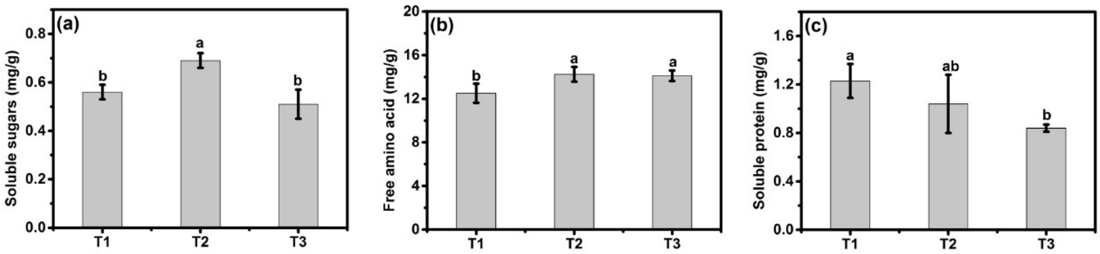

Figure 7S. the bio-active photochemistry of green-leaf pak-choi. (a) soluble sugars, (b) free amino acid, (c) soluble protein. Different letters indicate significant differences between treatments (a< 0.05).

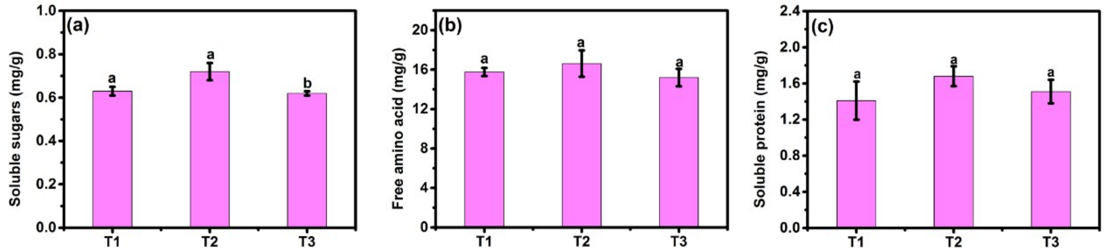

Figure 8S. the bio-active photochemistry of red-leaf pak-choi. (a) soluble sugars, (b) free amino acid, (c) soluble protein. Different letters indicate significant differences between treatments (a< 0.05).

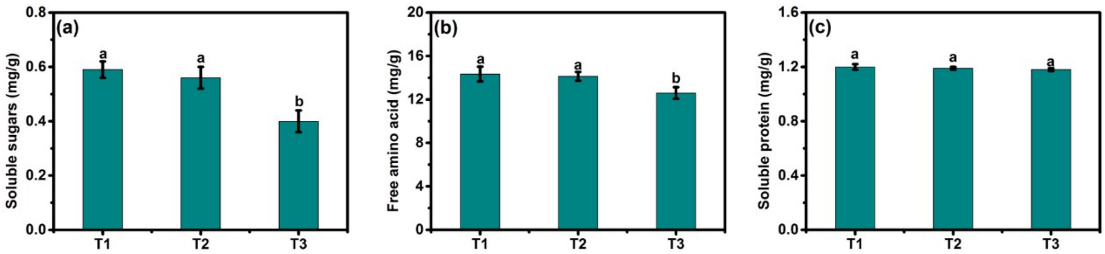

Figure 9S. the bio-active photochemistry of flowering Chinese cabbage. (a) soluble sugars, (b) free amino acid, (c) soluble protein. Different letters indicate significant differences between treatments (a< 0.05).

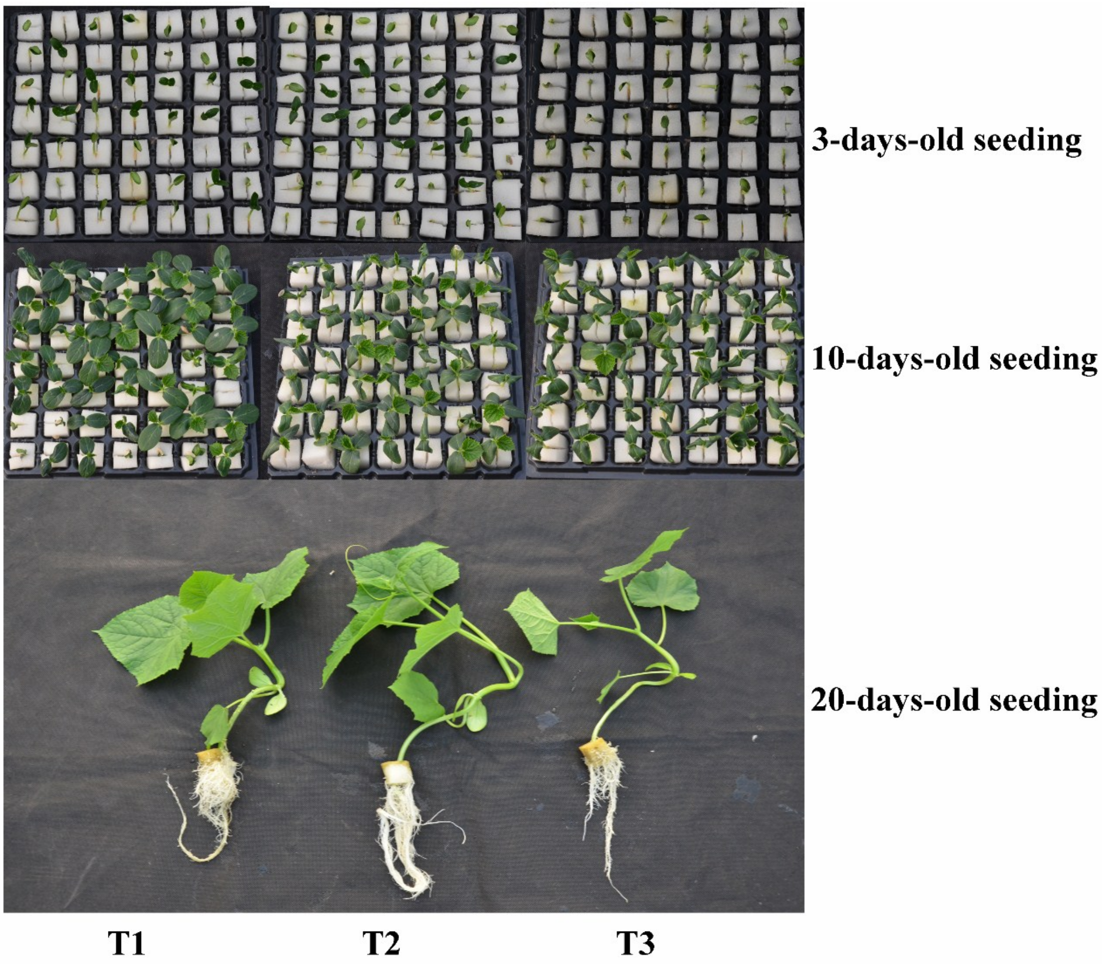

Figure 10S. The morphology of cucumber seeding on different physiology period.

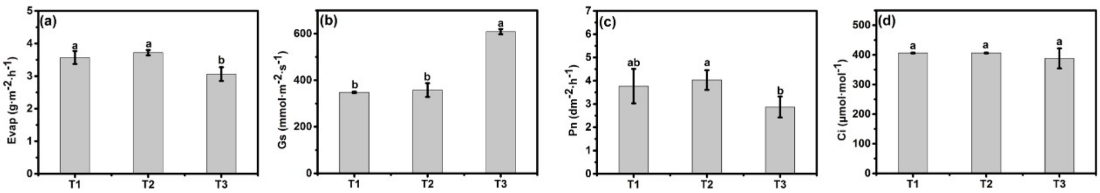

Figure 11S. the photosynthesis parameters of 20-days-old cucumber seeding under red:far-red radio. (a) Transportation Rate (Evap), (b) stomatal conductance (Gs), (c) Photosynthesis Rate (Pn), (d) intercellular CO_2 concentration (Ci). Different letters indicate significant differences between treatments (a< 0.05).

Table 3S. the biomass and morphology of 20-days-old cucumber seeding

	Overground fresh weight (mg/each plant)	Underground fresh weight (mg/each plant)	Overground dry weight (mg/each plant)	Underground dry weight (mg/each plant)
T1	4.60±0.83a	0.77±0.23a	0.23±0.05b	0.04±0.01b
T2	4.34±0.64a	0.82±0.19a	0.30±0.04a	0.07±0.01a
T3	3.53±0.6b	0.47±0.14b	0.27±0.05ab	0.03±0.01c
	Euphylla area (mm^2)	Stem diameter (cm)	Plant height (cm)	Hypocotyl length (cm)
T1	36.73±5.49a	0.39±0.04a	6.35±0.76b	3.41±0.54b
T2	32.55±4.56ab	0.35±0.05ab	6.82±1.09a	3.82±0.83ab
T3	3.82±0.83ab	0.34±0.04b	7.68±1.38a	4.30±0.66a

The values presented are the means ± SE. Different letters indicate significant differences between treatments (a< 0.05).

Notes and references

1. L. Huché-Thélier, L. Crespel and J. Gourrierec, *Environ. Exp. Bot.*, 2016, **121**, 22.
2. E. Burgie, N. Adam, M. Joseph, M. Duanmu, C. Bachy and S. Sudek, *PNAS*, 2014, **111**, 10179.
3. C. Sager, O. Smith and L. Edwards, *ASABE,* 1988, **31**, 1882.
4. J. Duan, S. Li and J. Kang, *Plant Physiol.*, 2008, **165**, 1620.
5. F. Ebell, *Phytochem.*, 1969, **8**, 227.
6. M. Bradford, *Anal. Biochem.*, 1976, **72**, 248.
7. A. Graser, G. Godel and S. Albers, *Anal. Biochem.,* 1985, **151**, 142.
8. T. Kozuka and A. Nagatani, *Plant Physiol.*, 2010, **153**, 1608.
9. M. Iwamoto and M. *Plant Physiol.,* 2011, **157**, 1187-1195.
10. Y. Kang, L. Lian and F. Wang, *Plant Cell*, 2009, **21**, 2624.
11. P. Lee and L. Lopez-Molina, *Cell Cycle*, 2012, **11**, 4489.
12. P. Lee, U. Piskurewicz and V. Turečková, *Genes & Development*, 2012, **26**, 1984.
13. M. Keller, Y. Jaillais and V. *Plant J. Cell Mol. Biol.*, 2011, **67**, 195.